

# Investigation of biosensor built with photonic crystal microcavity

Xiaoling Wang (王晓玲)<sup>1,2</sup>, Naiguang Lü (吕乃光)<sup>2</sup>, Qiaofeng Tan (谭峭峰)<sup>3</sup>, and Guofan Jin (金国藩)<sup>3</sup>

<sup>1</sup>*School of Electronic Engineering, Beijing University of Posts and Telecommunications, Beijing 100876*

<sup>2</sup>*School of Optoelectronic Information and Telecommunication Engineering, Beijing Information Science and Technology University, Beijing 100085*

<sup>3</sup>*State Key Laboratory of Precision Measurement Technology and Instruments, Tsinghua University, Beijing 100084*

Received September 16, 2008

The ultra-compact biosensor based on the two-dimensional (2D) photonic crystal (PhC) microcavity is investigated. The performances of the sensor are analyzed theoretically using the Fabry-Perot (F-P) cavity model and simulated using the finite-difference time-domain (FDTD) method. The simulation results go along with the theoretical analysis.

OCIS codes: 130.3990, 130.6010, 140.3945, 140.4780.

doi: 10.3788/COL20080612.0925.

Techniques used for the precise measurement of refractive index (RI) of gas and liquid are very useful methods due to the fact that the RI of the gas or liquid is related to its composition, pressure, density, and temperature. Especially, commercial label-free affinity-based optical biosensor detects selective binding by measuring the change of refractive index at the surface of the sensor<sup>[1–4]</sup>. These methods include surface plasmon resonance which attracts many studies recently, but it needs a relatively large sensing area ( $\sim 1$  mm), and it is not fit for the situations when the analyte is little and the sensor needs for integrating to other optical devices. Photonic crystals (PhC), which prohibit the propagation of light for frequencies within a band gap, have enabled exciting new ways to control light and open new possibilities for ultra-compact integrated optical devices.

Over the past few years, many reports about biosensors built with PhC were presented, including the PhC with waveguide structure<sup>[4]</sup>, microcavity structure, and the microcavity with sandwiched waveguide structure<sup>[5,6]</sup>. Because the small sensing area ( $\sim 10 \mu\text{m}^2$ ) of the device requires only  $\sim 1$  fL sample analyte, these ultra-compact biosensors would be used in the limited sample analyte in RI measurement<sup>[5]</sup> and the small sensing area would also allow dense integration of many sensors on the same chip and be fit for even single molecule detection<sup>[7]</sup>.

Among these new biosensors, the sensors with higher resolution of RI are achieved by the PhC microcavity. With the structure, we can achieve the better resolution of RI, higher transmittance efficiency, and wider measurement range of RI. In Ref. [6], using the PhC microcavity, the RI resolution of the sensor  $\Delta n$  is 0.001, transmission efficiency is relatively higher than 40%; the sensitivity of the sensor ( $\Delta\lambda/\Delta n$ ) is better than 300 nm/RIU (when lattice constant  $a = 440$  nm) with the measurement range of the RI about 1.0 – 1.6<sup>[6]</sup>, where RIU means the RI unit. In this letter, using the theoretical analysis, the performances of the biosensor are analyzed. The relations between the resonance wavelength and the RI of the analyte are achieved and those

between the sensors transmission efficiency and quality factor ( $Q$  factor) are also analyzed. The simulation results meet with the results of theoretical analysis.

The biosensor with a hexagonal lattice of air holes in the PhC is shown in Fig. 1. The input waveguide and output waveguide are obtained by removing one row of air holes and are used to couple light into and out of the PhC microcavity. The microcavity is formed by varying the radius of one air hole. The light emitted from the light source propagates through the input waveguide and is coupled to the output waveguide through the microcavity, and the corresponding transmission spectrum is detected by a spectrometer. The detected spectrum has a Lorentzian line shape in the PhC band gap when the PhC cavity is at resonance situation. When the PhC's air holes are full of analyte, the resonance wavelength of this sensor will shift accordingly due to the variation of the RI.

The defect radius of microcavity can be designed to have higher sensitivity to the ambient RI. The input waveguide and output waveguide are assigned to promote

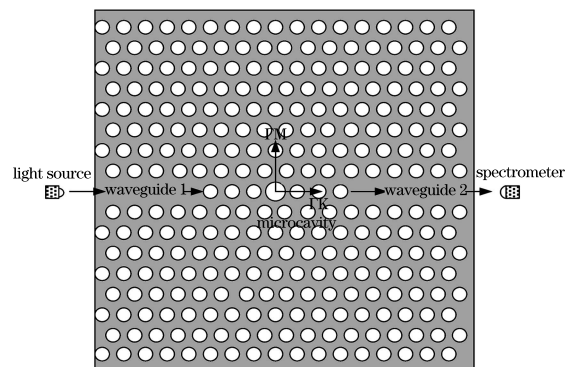


Fig. 1. Layout of the RI sensor based on 2D PhC with a hexagonal lattice of air holes. The structure consists of input waveguide (waveguide 1), microcavity, output waveguide (waveguide 2), coherent light source, and spectrometer.

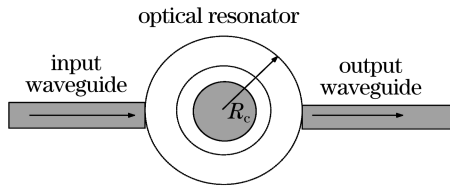


Fig. 2. Basic configuration of a sensor with a resonator between two waveguides.

the transmission efficiency. With a proper operating frequency, the structure can work as an ultra-compact biosensor with better sensitivity and higher transmission efficiency.

The sensor can be simplified as the structure shown in Fig. 2. The size of optical resonator varies with the radius of the cavity and so does the resonance mode. The resonator is somewhat like Fabry-Perot (F-P) sensor, in which the resonance also has a Lorentzian line shape. There is still main difference between them. Firstly, unlike traditional F-P cavity, it is a point defect PhC cavity in the sensor and the circle shape interface instead of the two plane segments in F-P cavity can be served as mirrors. Secondly, the PhC cavity with a constant size can support only one monopole mode and F-P supports a series of resonance frequency. Finally, the size of the cavity of the sensor is smaller than the operating wavelength, however a conventional F-P sensor can no longer function when the distance between the mirror is in that order of magnitude.

The resonance wavelength of F-P sensor can be expressed as<sup>[8]</sup>

$$\lambda_m = \frac{2nl}{m}, \quad (1)$$

where  $n$  is the RI of cavity between the mirrors,  $m$  is an integer,  $l$  is the length of cavity. In our PhC sensor with microcavity, the resonance frequency can be expressed as

$$\lambda_m = \frac{2nR}{m}, \quad (2)$$

where  $R$  can be defined as the parameter related with the cavity radius  $R_c$ . Here, what especially needs to be pointed is that  $R$  and  $R_c$  are not always proportional<sup>[6]</sup>. If the cavity radius (the center defect size) is more than the normal PhC air holes,  $R$  and  $R_c$  are proportional, and if it is less than that, they are inverse proportional.

Let the size of point defect constant, the parameters  $m$  and  $R$  are constants, and the resonance wavelength  $\lambda$  shifts with the PhC cavity index  $n$ . The shift of resonant wavelength satisfies

$$\Delta\lambda = \lambda_0 \frac{\Delta n}{n_0}, \quad (3)$$

where  $\Delta n$  is the change of RI of cavity,  $n_0$  is the initial RI of cavity,  $\lambda_0$  is the initial resonance wavelength of cavity.  $\Delta\lambda$  is the drift of  $\lambda_0$  when  $n_0$  changes to  $n_0 + \Delta n$ . If the microcavity of air holes is full of different analyte, the RI is varied and so is the resonance wavelength which is similar to the case of F-P sensor. Therefore the relation of  $\Delta\lambda$  and  $\Delta n$  is the linear relation.

Because the sensor's resolution is related with the

transmission efficiency and  $Q$  factor of the resonance, the transmission efficiency and the  $Q$  factor should be considered in the process of design. The transmission spectrum of the sensor has a Lorentzian line shape. In Lorentzian line shape, the transmission efficiency through the PhC resonance cavity for different frequencies can be expressed approximately as the following Lorentzian function<sup>[9]</sup>:

$$T(\omega, \omega_0) = \frac{\omega_0^2}{4Q^2(\omega - \omega_0)^2 + \omega_0^2}, \quad (4)$$

where  $\omega_0$  is the resonant frequency,  $Q$  is the quality factor of the resonant cavity. The transmission efficiency shifts with the change of PhC cavity  $Q$ . If the  $Q$  factor ( $Q > 1$ ) is increasing, the transmission efficiency is decreasing.

Based on the above theoretical analysis, a micro biosensor can be designed in a two-dimensional (2D) PhC with triangular lattice. The effective RI of the designed structure shown in Fig. 1 is 3.32 ( $\varepsilon = 11.0$ )<sup>[9]</sup>. The radius of air holes  $R$  is  $0.36a$ . Due to the dependence of the resonance mode on the defect size of microcavity<sup>[6]</sup>, the PhC cavity size should be designed carefully in order to realize high sensitivity and appropriate measurement range. The microcavity can be formed by varying the radius of the center air hole. The radius of the defect  $R_c$  can be limited from  $0.05a$  to  $0.55a$ . Through computing and comparing, the defect radius  $R_c$  is optimized as  $0.55a$  due to the fact that in the size, better sensitivity can be realized in RI measurement range of  $1.0 - 1.6$ <sup>[6]</sup>.

Using the finite-difference time-domain (FDTD) simulation, the relations between RI of the sensor and the change of wavelength are achieved. In Fig. 3, the resonance wavelength shift  $\Delta\lambda = \lambda(n) - \lambda(\text{air})$  is plotted as a function of ambient RI, and the sensor's sensitivity is  $\Delta\lambda/\Delta n = 330 \text{ nm/RIU}$  (lattice constant  $a = 440 \text{ nm}$ ) in the index measurement range  $1.0 - 1.6$ . The relation between the resonance frequency and the RI of the analyte is quasi-linear which goes along with the above theoretical analysis. The FDTD simulation result also shows that the resonance wavelength shifts up by  $\sim 0.4 \text{ nm}$  for  $\Delta n = 0.001$ .

The higher transmission efficiency can be realized by optimizing the parameters of the waveguides. In Fig. 4, when two holes are around the cavity, the transmission efficiency is high, but the  $Q$  factor is relatively low, as shown in Fig. 5. When four holes are selected, the  $Q$  factor is very high while transmission efficiency is very low. The relation between the transmission efficiency and the

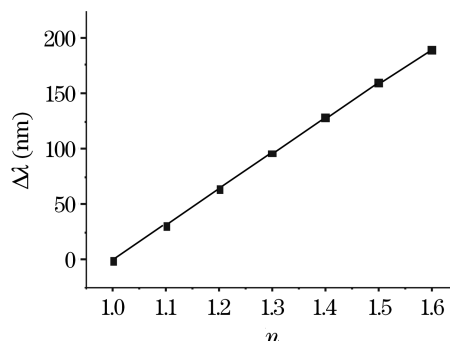


Fig. 3. Resonant wavelength shift  $\Delta\lambda$  plotted as a function of ambient index  $n$ .

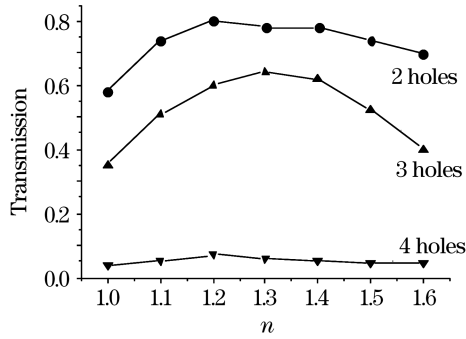


Fig. 4. Transmission of the sensor plotted as a function of ambient index  $n$  with different hole numbers around cavity.

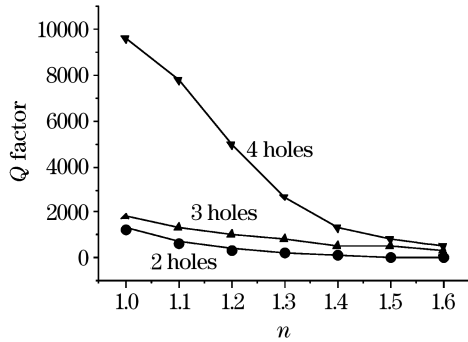


Fig. 5.  $Q$  factor plotted as a function of ambient index  $n$  with different hole numbers around cavity.

$Q$  factor is inverse proportional which fits for the theoretical analysis in Eq. (4). The number of air holes between the cavity and the waveguide can be chosen as three because of the transmission efficiency and the  $Q$  factor are all relatively high.

The sensor's resolution is also affected by the  $Q$  factor and transmission efficiency. With the optimum structure, the  $Q$  factor can achieve 700 – 3820 and the transmission efficiency can reach about 0.54–0.90 in the index

range of 1.0 – 1.6, and these parameters should meet the resolution need of detection of the sensor<sup>[5]</sup>.

In summary, we have investigated the biosensor based on the 2D PhC microcavity. Using the theoretical analysis model which is similar to the Fabry-Perot cavity, the performances of the RI sensor are analyzed. The relations between the resonance wavelength and the RI of the analyte are quasi-linear, and that between the sensor's transmission efficiency and  $Q$  factor are inverse proportional. The simulation results meet with the theoretical analysis. The sensor can be used to measure gas, fluids, biolayers, or bound chemicals due to the wide measurement range.

This work was supported by the National Basic Research Program of China (No. 2007CB935303) and the Electromechanical System and Measurement and Control Program of Beijing Municipal Key Laboratory (No. 82063010). The authors would like to acknowledge the Tsinghua-Foxconn Nanotechnology Research Center. X. Wang's e-mail address is wangxiaoling66@gmail.com.

## References

1. S.-Y. Wu and H. Ho, *Chin. Opt. Lett.* **6**, 176 (2008).
2. B. Cunningham, P. Li, B. lin, and J. Pepper, *Sensors and Actuators B* **81**, 316 (2002).
3. V. S.-Y. Lin, K. Motesharei, K.-P. S. Dancil, M. J. Sailor, and M. R. Ghadiri, *Science* **278**, 840 (1997).
4. F. Morhard, J. Pipper, R. Dahint, and M. Grunze, *Sensors and Actuators B* **70**, 232 (2000).
5. E. Chow, A. Grot, L. W. Mirkarimi, M. Sigalas, and G. Girolami, *Opt. Lett.* **29**, 1093 (2004).
6. X. Wang, Z. Xu, N. Lu, J. Zhu, and G. Jin, *Opt. Commun.* **281**, 1725 (2008).
7. M. Lee and P. M. Fauchet, *Opt. Express* **15**, 4530 (2007).
8. H. A. Haus, *Waves and Fields in Optoelectronics* (Prentice-Hall, Englewood Cliffs, 1985) p.68.
9. Z. Xu, L. Cao, C. Gu, Q. He, and G. Jin, *Opt. Express* **14**, 298 (2006).